Synchronous Controller for Identical Synchronization in Networks with Arbitrary Topological Structure of n Reaction-Diffusion Systems of the Hindmarsh-Rose 3D Type

Phan Van Long Em

***Abstract*—This paper investigates identical synchronization in networks composed of n reaction-diffusion systems of the Hindmarsh-Rose 3D type with arbitrary topological structures. We design a controller for these networks aimed at achieving the desired synchronization, with the synchronization error defined in $\mathbb{R}$. The effectiveness of this controller is demonstrated through theoretical proofs. Additionally, we present numerical results to further validate the theoretical findings.**

***Index Terms*—Hindmarsh-Rose 3D model, identical synchronization, networks with arbitrary topological structure, reaction-diffusion systems.**

I. Introduction

SYNCHRONIZATION has been extensively studied across various fields and natural phenomena [1], [3], [4], [5], [6], [7], [8]. Mathematically, "synchronization" refers to different systems exhibiting the same behavior at the same time [1]. In recent years, there has been a growing interest in complex dynamical networks due to their large-scale applicability in domains such as information processing, the World Wide Web, biological systems, and neural networks [20], [21], [22], [23].

Synchronization is regarded as a fundamental problem in cooperative control, requiring all subsystems within a network to converge to a target state or a common value. This phenomenon is commonly referred to as identical synchronization, and most theoretical research on synchronization in complex networks has focused on this aspect [1], [2], [10], [11], [15], [16], [18].

Additionally, most of these studies have examined identical synchronization in networks with specific structures, such as fully connected networks [15], [16], hierarchical networks [18], and chain networks [10]. However, these idealized structures are rarely found in real-world scenarios. Instead, networks with arbitrary structures are more commonly encountered and provide a closer representation of real neural networks (for example, see Fig. 1).

Motivated by the discussion above, this paper aims to improve upon previous work by identifying sufficient conditions for achieving identical synchronization in networks composed of n reaction-diffusion systems of the Hindmarsh-Rose 3D type with arbitrary topological structures.

Manuscript received November 30, 2024; revised February 13, 2025.

This research is funded by An Giang University (AGU), Vietnam National University HoChiMinh City (VNU-HCM) under grant number 25.01.SP.

Phan Van Long Em is a lecturer of An Giang University, Vietnam National University, Ho Chi Minh City, VIETNAM (e-mail: pvlem@agu.edu.vn).

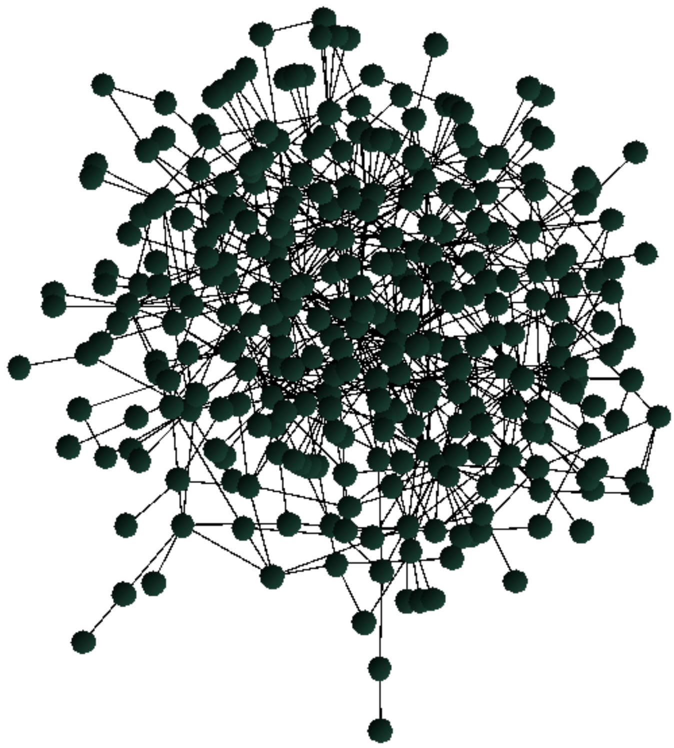

Fig. 1. An example of networks with arbitrary topological structure.

Additionally, we focus on obtaining identical synchronization with the synchronization error defined in $\mathbb{R}$. It is important to note that all results obtained in prior studies [10], [11], [15], [16], [18] defined the synchronization error in the function space $L^2(\Omega)$, where $L^2(\Omega)$ is based on a natural generalization of the 2-norm for finite-dimensional vector spaces, and $\Omega \subset \mathbb{R}^N$ with N as a positive integer. This represents a significant improvement over previously published results. However, due to the arbitrary nature of the network topologies and the synchronization error being defined in $\mathbb{R}$, achieving the desired outcomes presents certain challenges since the presence of the Laplace operator in each subsystem of the network complicates the situation.

To address this, we propose a controller that can be strategically placed within the network to mitigate the influence of the Laplace operator when calculating the synchronization error in $\mathbb{R}$. Furthermore, we present numerical results to validate the effectiveness of our theoretical findings.

II. Identical synchronization in networks with arbitrary topological structure of n reaction-diffusion systems of the Hindmarsh-Rose 3D type

In 1952, A. L. Hodgkin and A. F. Huxley published a paper introducing a mathematical model consisting of four ordinary differential equations that approximated certain properties of neuronal membrane potential [2], [7], [4]. Their remarkable work earned them a Nobel Prize. Building on their foundational study, many scientists sought to simplify the Hodgkin-Huxley model while preserving the essential energizing and biological properties of the cell. Among these researchers were J. L. Hindmarsh and R. M. Rose, who introduced the Hindmarsh-Rose 3D model in 1984 [7], [9]. This model comprises three ordinary differential equations that simplify Hodgkin-Huxley's system and help describe neuronal voltage dynamics [6].

The model includes two primary variables, u and v, as well as a third variable w. The first variable, $u = u(t)$, represents the transmembrane voltage of the cell, while $v = v(t)$ and $w = w(t)$ account for various physical quantities, such as the electrical conductivity of ion currents across the membrane. The ordinary differential equations that define the Hindmarsh-Rose 3D model are detailed below [2], [7], [9]:

$$\begin{cases} \dfrac{du}{dt} = u_t = f(u) + v - w + I, \\ \\ \dfrac{dv}{dt} = v_t = 1 - bu^2 - v, \\ \\ \dfrac{dw}{dt} = w_t = r(s(u-c) - w), \end{cases} \tag{1}$$

where $f(u) = -u^3 + au^2$; a, b, c, r, s are constants $(a, b, r, s > 0)$; I presents the external current; t presents the time.

The system (1) is inadequate for accurately capturing the propagation of action potentials. To resolve this issue, we will apply the cable equation to enhance our model by incorporating the Laplace operator into the first equation of the system (1). This addition allows us to effectively describe the propagation of action potentials. Furthermore, this mathematical framework is based on a circuit representation of the cell membrane, which includes both the intracellular and extracellular spaces. It provides a quantitative analysis of current flow and voltage changes within and between neurons. This approach enables us to achieve a comprehensive understanding of cellular function, both quantitatively and qualitatively. Consequently, we will consider the reaction-diffusion system of the Hindmarsh-Rose 3D type (HR), which is as follows:

$$\begin{cases} u_t = f(u) + v - w + I + d\Delta u, \\ v_t = 1 - bu^2 - v, \\ w_t = r(s(u-c) - w), \end{cases} \tag{2}$$

where $u = u(x,t),\ v = v(x,t),\ w = w(x,t),\ (x,t) \in \Omega \times \mathbb{R}^+$, d is a positive constant, Δu is the Laplace operator of u, $\Omega \subset \mathbb{R}^N$ is a regular bounded open set with Neumann zero flux boundary conditions, and N is a positive integer. This model allows the appearance of many patterns and relevant phenomena in physiology, and presents the distribution of the membrane potential along the axon of a single cell [6], [7]. Hereafter, system (2) is considered as a neural model, and a network of n coupled systems (2) is constructed as follows:

$$\begin{cases} u_{it} = f(u_i) + v_i - w_i + I + d\Delta u_i + \sum\limits_{j=1}^{n} c_{ij} h(u_i, u_j), \\ v_{it} = 1 - bu_i^2 - v_i, \\ w_{it} = r(s(u_i - c) - w_i), \\ i, j = 1, ..., n, i \neq j, \end{cases} \tag{3}$$

where $(u_i, v_i, w_i), i = 1, 2, ..., n$, is defined as in (2). The coefficients c_{ij} are the elements of the connectivity matrix $C_n = (c_{ij})_{n \times n}$, defined by: $c_{ij} > 0$ if neuron ith and jth are coupled, $c_{ij} = 0$ if neuron ith and jth are not coupled, and $c_{ii} = -\sum\limits_{j \neq i, j=1}^{n} c_{ij}$, where $i, j = 1, 2, ..., n, i \neq j$. This matrix also illustrates the network topology. The function h describes the coupling function, which defines the type of connection between the i-th and j-th cells. As is well known, neurons connect via synapses, resulting in two types of connections between cells: chemical and electrical. Mathematically, when neurons are connected through chemical synapses, the coupling function is nonlinear [10], [11], [2] and is expressed by the following formula:

$$\begin{cases} h(u_i, u_j) = -g_{syn}(u_i - V_{syn}) \dfrac{1}{1 + \exp(-\lambda(u_j - \theta_{syn}))}, \\ i = 1, 2, ..., n, \end{cases} \tag{4}$$

where $u_j, j = 1, 2, ..., n$, presents the node jth connected to the node ith; g_{syn} is a positive number and represents the coupling strength; V_{syn} is the reversal potential and must be larger than $u_i(x,t)$, for all $i = 1, 2, ..., n$, and $x \in \Omega, t \geq 0$ since synapses are supposed excitatory; θ_{syn} is the threshold reached by every action potential for a neuron; λ is a positive number [2], [14]. The bigger λ is and the better we approach the Heaviside function.

If the neurons connect through electrical synapses, the coupling function is linear [2], [15] and is described by the following formula:

$$h(u_i, u_j) = -g_{syn}(u_i - u_j),\ i, j = 1, 2, ..., n, \tag{5}$$

where g_{syn} is positive number presenting the coupling strength.

To achieve identical synchronization in the network described in (3), we need to reformulate this system as follows:

$$\begin{cases} u_{1t} = f(u_1) + v_1 - w_1 + I + d\Delta u_1 + \sum\limits_{j=1}^{n} c_{1j} h(u_1, u_j), \\ v_{1t} = 1 - bu_1^2 - v_1, \\ w_{1t} = r(s(u_1 - c) - w_1), \\ u_{it} = f(u_i) + v_i - w_i + I + d\Delta u_i + \sum\limits_{m=1}^{n} c_{im} h(u_i, u_m), \\ v_{it} = 1 - bu_i^2 - v_i, \\ w_{it} = r(s(u_i - c) - w_i), \\ i = 2, 3, ..., n, , i \neq 1, i \neq m, j \neq 1. \end{cases} \tag{6}$$

The definition of identical synchronization is as follows:

Definition 1 (see [1], [11]). Let $\sum\limits_{i=2}^{n} |e_i^u| + |{e^v}_i| + |e_i^w|$ be the identical synchronization error, where $e_i^u = u_i - u_1, e_i^v =$

$v_i - v_1, e_i^w = w_i - w_1$, for all $i = 2, ..., n$. We say that the network (6) achieves identical synchronization if the synchronization error approaches zero as time t approaches infinity.

Before presenting the main results, we need to consider the following remark that assists in proving our desired outcomes.

Remark 1 (see [19])**.** The function f satisfies the following condition:

$$|f(u_i) - f(u_j)| \leq \alpha |u_i - u_j|, \; i, j = 1, 2, ..., n, \quad (7)$$

where u_i, u_j present the transmembrane voltages, and α is a positive number.

Remark 2 (see [19])**.** The function h defined by (4) and (5) satisfies the following condition:

$$\begin{cases} |h(u_i, u_k) - h(u_j, u_l)| \leq \beta |u_i - u_j|, \\ i, j, k, l = 1, 2, ..., n, i \neq k, j \neq l, \end{cases} \quad (8)$$

where u_i, u_j, u_k, u_l present the transmembrane voltages, and β is a positive number.

In this work, we aim to investigate the sufficient conditions for achieving identical synchronization in the network described by system (6), where the identical synchronization error is defined in $\mathbb{R}$. However, the presence of the Laplace operator for u_i (for all $i = 1, 2, \ldots, n$) complicates this goal. To address this challenge, the author proposes the introduction of a controller at node i (for $i \neq 1$) within the network (6). This controller is designed to mitigate the effects of the Laplace operator and facilitate identical synchronization, with the synchronization error still defined in $\mathbb{R}$. With this approach, the network (6), after the addition of the controller denoted as Γ_i (for $i = 2, 3, \ldots, n$), can be expressed as follows:

$$\begin{cases} u_{1t} = f(u_1) + v_1 - w_1 + I + d\Delta u_1 + \sum\limits_{j=2}^{n} c_{1j} h(u_1, u_j), \\ v_{1t} = 1 - bu_1^2 - v_1, \\ w_{1t} = r(s(u_1 - c) - w_1), \\ u_{it} = f(u_i) + v_i - w_i + I + d\Delta u_i \\ \qquad\qquad + \sum\limits_{m=1}^{n} c_{im} h(u_i, u_m) + \Gamma_i, \\ v_{it} = 1 - bu_i^2 - v_i, \\ w_{it} = r(s(u_i - c) - w_i), \\ i = 2, 3, ..., n, , i \neq 1, i \neq m, j \neq 1, \end{cases} \quad (9)$$

where the controller $\Gamma_i = \Gamma_i(x, t)$ is designed as follows:

$$\begin{aligned} \Gamma_i = & -d\Delta u_i + d\Delta u_1 - \sum_{m=1, m\neq i}^{n} c_{im} h(u_1, u_m) \\ & + \sum_{j=2}^{n} c_{1j} h(u_1, u_j) - k_i e_i^u, \end{aligned} \quad (10)$$

with the updated rules defined as follows:

$$k_{it} = r_i (e_i^u)^2, \quad (11)$$

where $k_i = k_i(x, t)$; r_i is a arbitrary positive constant, for all $i = 2, ..., n$.

Under the action of the controller designed as above, the error dynamic equations of the system (9) are described as:

$$\begin{aligned} e_{it} &= (u_{it} - u_{1t}) \\ &= f(u_i) + v_i - w_i + I + d\Delta u_i + \sum_{m=1, m\neq i}^{n} c_{im} h(u_i, u_m) \\ &\quad + \Gamma_i - f(u_1) - v_1 + w_1 - I - d\Delta u_1 - \sum_{j=2}^{n} c_{1j} h(u_1, u_j) \\ &= f(u_i) - f(u_1) + e_i^v - e_i^w \\ &\quad + \sum_{m=1, m\neq i}^{n} c_{im} (h(u_i, u_m) - h(u_1, u_m)) - k_i e_i^u, \end{aligned} \quad (12)$$

$$\begin{aligned} e_{it}^v &= v_{it} - v_{1t} = 1 - bu_i^2 - v_i - (1 - bu_1^2 - v_1) \\ &= -b(u_i + u_1) e_i^u - e_i^v, \end{aligned} \quad (13)$$

and

$$\begin{aligned} e_{it}^w &= w_{it} - w_{1t} = rs(u_i - c) - rw_i - rs(u_1 - c) + rw_1 \\ &= rs(u_i - u_1) - r(w_i - w_1) \\ &= rse_i^u - re_i^w, \end{aligned} \quad (14)$$

for $i = 2, ..., n$.

Next, we explore the sufficient condition for the identical synchronization problem of network (9). The main result is presented in the following theorem.

Theorem 1. *The network* (9) *identically synchronizes with the identical synchronization error in* $\mathbb{R}$ *under the adaptive controllers* (10) *and updated rules* (11).

Proof: To prove this theorem , we construct the Lyapunov function as follows:

$$V(x, t) = \frac{1}{2} \sum_{i=2}^{n} \left((e_i^u)^2 + (e_i^v)^2 + \frac{1}{rs} (e_i^w)^2 + \frac{1}{r_i} (k_i - k)^2 \right), \quad (15)$$

where k is a positive constant to be determined.

By calculating the time derivative of $V(x, t)$ along the error systems (12), (13) and (14), we get:

$$\begin{aligned} \frac{\partial V(x, t)}{\partial t} &= \sum_{i=2}^{n} \left[e_i^u e_{it}^u + e^v{}_i e^v{}_{it} + \frac{1}{rs} e_i^w e_{it}^w + \frac{1}{r_i} (k_i - k) k_{it} \right] \\ &= \sum_{i=2}^{n} [e_i^u (f(u_i) - f(u_1) - e^v{}_i - e_i^w - k_i e_i^u) \\ &\quad + e_i^u \sum_{m=1, m\neq i}^{n} c_{im} (h(u_i, u_m) - h(u_1, u_m)) \\ &\quad e_i^v (-b(u_i + u_1) e_i^u - e_i^v) + \frac{1}{rs} e_i^w (rse_i^u - re_i^w) \\ &\quad + (k_i - k)(e_i^u)^2] \\ &= \sum_{i=2}^{n} [e_i^u (f(u_i) - f(u_1)) + e_i^u e_i^v \\ &\quad - be_i^u e_i^v (u_i + u_1) \\ &\quad + e_i^u \sum_{m=1, m\neq i}^{n} c_{im} (h(u_i, u_m) - h(u_1, u_m)) \\ &\quad \left. - \frac{1}{s} (e_i^w)^2 - (e_i^v)^2 - k(e_i^u)^2 \right]. \end{aligned} \quad (16)$$

By using Remarks 1-2, it is easy to obtain:

$$\begin{aligned}\frac{\partial V(x,t)}{\partial t} &\leq \sum_{i=2}^{n}\Big[\alpha(e_i^u)^2+|e_i^u|.|e_i^v|(1+b(|u_i|+|u_1|))\\ &+\sum_{m=1,m\neq i}^{n}\beta|c_{im}|(e_i^u)^2-\frac{1}{s}(e_i^w)^2-(e_i^v)^2-k(e_i^u)^2\Big]\\ &\leq \sum_{i=2}^{n}\Big[\alpha(e_i^u)^2+|e_i^u|.|e_i^v|(1+b(|u_i|+|u_1|))\\ &\quad+\beta(n-1)\max_{1\leq m\leq n,m\neq i}|c_{im}|(e_i^u)^2\\ &\quad-\frac{1}{s}(e_i^w)^2-(e_i^v)^2-k(e_i^u)^2\Big].\end{aligned} \tag{17}$$

By using the Young's inequality for every $\delta > 0$, we can see:

$$\begin{aligned}&|e_i^u|\,|e^v{}_i|\,(1+b(|u_i|+|u_1|))\leq\\ &\leq(1+b(|u_i|+|u_1|))(\frac{1}{2\delta}(e_i^u)^2+\frac{\delta}{2}(e_i^v)^2)\\ &\leq\frac{M}{2\delta}(e_i^u)^2+\frac{M\delta}{2}(e_i^v)^2,\end{aligned} \tag{18}$$

where M is a positive constant, since $u_i, i = 1, 2, ..., n$ are bounded (see [17]).

Combining (17)-(18) yields:

$$\begin{aligned}\frac{\partial V(x,t)}{\partial t} &\leq \sum_{i=2}^{n}\Big[\alpha(e_i^u)^2+\frac{M}{2\delta}(e_i^u)^2+\frac{M\delta}{2}(e_i^v)^2\\ &\quad+\beta(n-1)\max_{1\leq m\leq n,m\neq i}|c_{im}|(e_i^u)^2\\ &\quad-\frac{1}{s}(e_i^w)^2-(e_i^v)^2-k(e_i^u)^2\Big]\\ &\leq\sum_{i=2}^{n}\Big[(\alpha+\frac{M}{2\delta}+\beta(n-1)\max_{1\leq m\leq n,m\neq i}|c_{im}|-k)(e_i^u)^2\\ &\quad(\frac{M\delta}{2}-1)(e_i^v)^2-\frac{1}{s}(e_i^w)^2\Big].\end{aligned} \tag{19}$$

We choose $\delta < \dfrac{2}{M}$ and

$$k > \alpha+\frac{M}{2\delta}+\beta(n-1)\max_{1\leq m\leq n,m\neq i}|c_{im}|,$$

then (19) can be estimated as:

$$\frac{\partial V(x,t)}{\partial t}\leq-\gamma\frac{1}{2}\sum_{i=2}^{n}\left((e_i^u)^2+(e_i^v)^2+\frac{1}{rs}(e_i^w)^2\right), \tag{20}$$

where

$$\gamma=\min\Big\{2(k-\alpha-\frac{M}{2\delta}-\beta(n-1)\max_{1\leq m\leq n,m\neq i}|c_{im}|),\ 2(1-\frac{M\delta}{2}),2r\Big\}.$$

From (20), it can be seen that $0 \leq V(x,t) \leq V(x,0)$, this together with (15) implies that $V(x,t)$ is bounded. It is based on Lyapunov stability theory and LaSalle's invariance principle [13], we have:

$$\lim_{t\to+\infty}\sum_{i=2}^{n}|e_i^u|+|e^v{}_i|+|e_i^w|=0.$$

Therefore, it implies that the network (9) achieves identical synchronization in the sense of Definition 1. The theorem is proved. ■

III. Numerical results and discussion

In this section, we present specific examples to evaluate the effectiveness of the proposed method discussed in the theoretical section for two cases: $\Omega \subset \mathbb{R}$ and $\Omega \subset \mathbb{R}^2$. The integration is conducted using R. The simulation results were obtained with the following parameter values [14], [2], [15], [16]:

$$f(u)=-u^3+au^2, a=3, b=5, s=4, r=0.008,$$
$$c=-\frac{1}{2}(1+\sqrt{5}), I=3.25, d=0.05,$$
$$\lambda=10,\ V_{syn}=2,\ \theta_{syn}=-0,25.$$

A. Example 1.

In this example, we examine a chain network consisting of two nodes that are linearly coupled. We will construct a controller, as described in the theoretical section, to achieve identical synchronization. Specifically, the system representing this chain network of two neurons with linear coupling is outlined below:

$$\begin{cases}u_{1t}=f(u_1)+v_1-w_1+I+d\Delta u_1,\\ v_{1t}=1-bu_1^2-v_1,\\ w_{1t}=r(s(u_1-c)-w_1),\\ u_{2t}=f(u_2)+v_2-w_2+I+d\Delta u_2-g_{syn}(u_2-u_1),\\ v_{2t}=1-bu_2^2-v_2,\\ w_{2t}=r(s(u_2-c)-w_2).\end{cases} \tag{21}$$

Now, we construct a controller for this network as follows:

$$\begin{cases}u_{1t}=f(u_1)+v_1-w_1+I+d\Delta u_1,\\ v_{1t}=1-bu_1^2-v_1,\\ w_{1t}=r(s(u_1-c)-w_1),\\ u_{2t}=f(u_2)+v_2-w_2+I+d\Delta u_2\\ \qquad\qquad -g_{syn}(u_2-u_1)+\Gamma_2,\\ v_{2t}=1-bu_2^2-v_2,\\ w_{2t}=r(s(u_2-c)-w_2),\end{cases} \tag{22}$$

where the controller Γ_2 is designed as follows:

$$\Gamma_2=-d\Delta u_2+d\Delta u_1-k_2e_2^u, \tag{23}$$

with the updated rule defined as follows:

$$k_{2t}=r_2(e_2^u)^2, \tag{24}$$

where r_2 is a arbitrary positive constant.

Note that (23) and (24) are constructed as the proposed controller (10) and the updated rule (11).

Let $|e_2^u|+|e_2^v|+|e_2^w| = |u_2-u_1|+|v_2-v_1|+|w_2-w_1|$ be the identical synchronization error of the network (22). We say that this network identically synchronizes if the identical synchronization error reaches zero as t approaches infinity.

First, we check the effectiveness of the proposed controller for this example in the following domain:

$$[0;T]\times\Omega=[0;5000]\times[0;100],$$

i.e., $\Omega \subset \mathbb{R}$ with Neumann zero flux boundary conditions. Besides, the initial conditions for the first node are defined as follows:

$$u_1(x,0)=1+\sin(2\pi x),$$
$$v_1(x,0)=1+\sin(2\pi x),$$
$$w_1(x,0)=1+\sin(2\pi x),$$

for all $x \in \Omega$.

The initial conditions for the second node are set so that the value is 0 everywhere, except for the central point, where we assign a value of 1.

Fig. 2 illustrates the identical synchronization errors of the network described by system (21) with a coupling strength of $g_{syn} = 0.0005$. In Fig. 2(a), we simulate the network without the controller defined in (23) and the updated rule in (24). The simulation results indicate that the identical synchronization error does not converge to zero, which implies that the identical synchronization phenomenon does not occur.

Furthermore, Fig. 3 displays the time series of all variables within the system defined by (21), without the controller in (23) and the updated rule in (24). In Fig. 3(a), the variable u_1 is represented by a solid line, while u_2 is shown by a dotted line. Similarly, in Fig. 3(b), v_1 and v_2 are presented in this manner, and in Fig. 3(c), w_1 and w_2 follow the same format. It is evident that the solid lines do not replicate the behavior of the dotted lines, further supporting the conclusion that identical synchronization does not occur in this scenario.

In Fig. 2(b), we simulate the network described by (21), using the controller specified in (23) and the updated rule in (24), with $r_2 = 0.2$. The results demonstrate that the synchronization error between the systems reaches zero, indicating that:

$$u_1(x,t) \approx u_2(x,t),$$
$$v_1(x,t) \approx v_2(x,t),$$
$$w_1(x,t) \approx w_2(x,t).$$

Fig. 4 illustrates the time series for all variables in the system defined by (21), under the control of (23) and the updated rule (24). In Fig. 4(a), the variable u_1 is represented by the solid line, while u_2 is depicted with a dotted line. Similarly, v_1 and v_2 are shown in Fig. 4(b), and w_1 and w_2 in Fig. 4(c). It is evident that the solid lines replicate the behavior of the dotted ones, confirming that the identical synchronization phenomenon occurs in this case.

Next, we check the effectiveness of the proposed controller for this example in the following domain:

$$[0;T] = [0;500]\,;\ \Omega = [0;1] \times [0;1]\,,$$

i.e., $\Omega \subset \mathbb{R}^2$ with Neumann zero flux boundary conditions. Besides, the initial conditions for the first node are defined as follows:

$$u_1(x,0) = -(x_1 - 0.5)^2 - (x_2 - 0.5)^2,$$
$$v_1(x,0) = -(x_1 - 0.5)^2 - (x_2 - 0.5)^2,$$
$$w_1(x,0) = -(x_1 - 0.5)^2 - (x_2 - 0.5)^2,$$

for all $x = (x_1, x_2) \in \Omega$.

The initial conditions for the second node are defined as follows:

$$u_2(x,0) = -x_1^2 - x_2^2,$$
$$v_2(x,0) = -x_1^2 - x_2^2,$$
$$w_2(x,0) = -x_1^2 - x_2^2,$$

for all $x = (x_1, x_2) \in \Omega$.

Fig. 5 represents the identical synchronization errors of the network (21) with respect to the coupling strength $g_{syn} = 0.0005$. Specifically, in Fig. 5(a), we simulate the network (21) without controller (23) and the updated rule (24). The simulation shows that the identical synchronization error does not reach zero, which means the identical synchronization phenomenon does not occur. Clearly, Fig. 6 represents the patterns of all state variables of the system (21) without controller (23) and the updated rule (24) in Ω. Specifically, Fig. 6(a) represents the pattern of $u_1(x,500)$, for all $x = (x_1, x_2) \in \Omega$ (respectively, $v_1(x,500)$ in Fig. 6(b); $w_1(x,500)$ in Fig. 6(c); $u_2(x,500)$ in Fig. 6(d); $v_2(x,500)$ in Fig. 6(e); $w_2(x,500)$ in Fig. 6(f)). We can see that the pattern of $u_1(x,500)$ and the pattern of $u_2(x,500)$ are not the same (respectively, $v_1(x,500)$ and $v_2(x,500)$; $w_1(x,500)$ and $w_2(x,500)$). In other words, the identical synchronization phenomenon does not occur in this case.

However, in Fig. 5(b), we simulate the network (21) with controller (23) and the updated rule (24), i.e., the system (22). The simulation shows that the identical synchronization error reaches zero, which means:

$$u_1(x,t) \approx u_2(x,t),\ v_1(x,t) \approx v_2(x,t),\ w_1(x,t) \approx w_2(x,t).$$

Fig. 7 represents the patterns of all state variables of the system (21) with controller (23) and the updated rule (24) in Ω. Specifically, Fig. 7(a) represents the pattern of $u_1(x,500)$, for all $x = (x_1, x_2) \in \Omega$ (respectively, $v_1(x,500)$ in Fig. 7(b); $w_1(x,500)$ in Fig. 7(c); $u_2(x,500)$ in Fig. 7(d); $v_2(x,500)$ in Fig. 7(e); $w_2(x,500)$ in Fig. 7(f)). We can see that the pattern of $u_1(x,500)$ and the pattern of $u_2(x,500)$ are the same (respectively, $v_1(x,500)$ and $v_2(x,500)$; $w_1(x,500)$ and $w_2(x,500)$). In other words, the identical synchronization phenomenon occurs in this case.

B. Example 2.

In this example, we examine a full network consisting of two nodes with nonlinear coupling and design a controller, as described in the theoretical section, to achieve identical synchronization. Specifically, the system representing a full network of two neurons with nonlinear coupling is outlined as follows:

$$\begin{cases} u_{1t} = f(u_1) + v_1 - w_1 + I + d\Delta u_1 \\ \qquad\qquad -g_{syn}(u_1 - V_{syn}) \dfrac{1}{1 + \exp(-\lambda(u_2 - \theta_{syn}))}, \\ v_{1t} = 1 - bu_1^2 - v_1, \\ w_{1t} = r(s(u_1 - c) - w_1), \\ u_{2t} = f(u_2) + v_2 - w_2 + I + d\Delta u_2 \\ \qquad\qquad -g_{syn}(u_2 - V_{syn}) \dfrac{1}{1 + \exp(-\lambda(u_1 - \theta_{syn}))}, \\ v_{2t} = 1 - bu_2^2 - v_2, \\ w_{2t} = r(s(u_2 - c) - w_2). \end{cases} \tag{25}$$

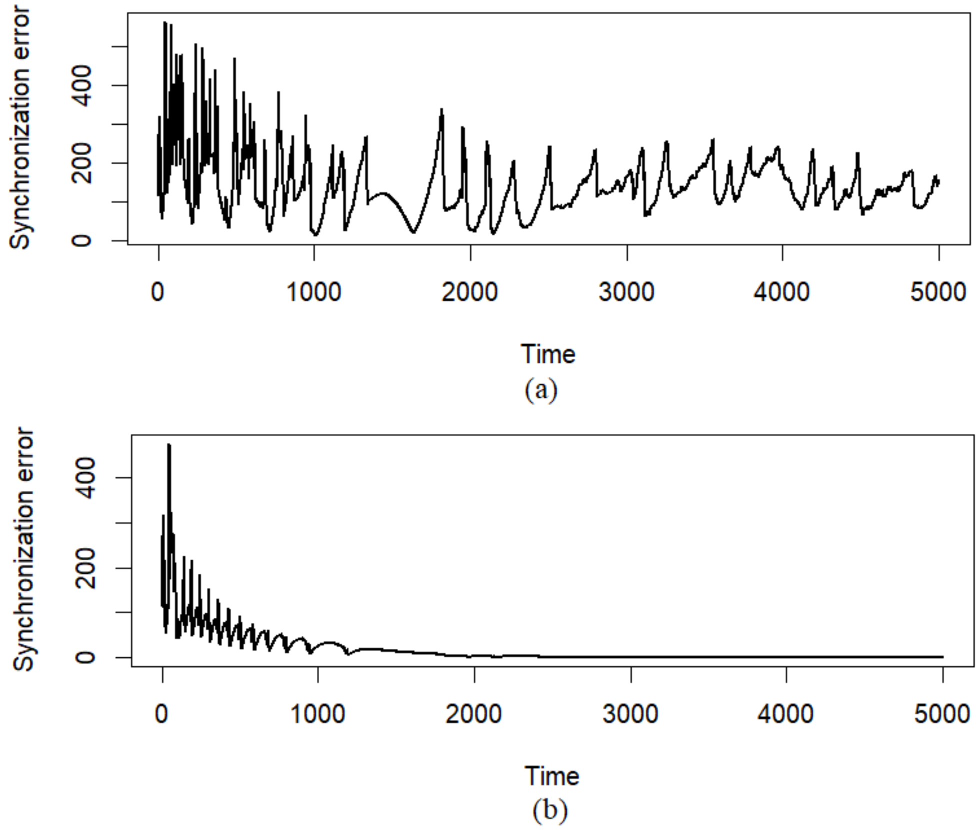

Fig. 2. Identical synchronization errors in the network described by (21) with a coupling strength of $g_{syn} = 0.0005$, $\Omega = [0; 100] \subset \mathbb{R}$.

Now, we construct a controller for this network as follows:

$$\begin{cases} u_{1t} = f(u_1) + v_1 - w_1 + I + d\Delta u_1 \\ \qquad -g_{syn}(u_1 - V_{syn}) \dfrac{1}{1 + \exp(-\lambda(u_2 - \theta_{syn}))}, \\ v_{1t} = 1 - bu_1^2 - v_1, \\ w_{1t} = r(s(u_1 - c) - w_1), \\ u_{2t} = f(u_2) + v_2 - w_2 + I + d\Delta u_2 \\ \qquad -g_{syn}(u_2 - V_{syn}) \dfrac{1}{1 + \exp(-\lambda(u_1 - \theta_{syn}))} + \Gamma_2, \\ v_{2t} = 1 - bu_2^2 - v_2, \\ w_{2t} = r(s(u_2 - c) - w_2), \end{cases} \tag{26}$$

where the controller Γ_2 is designed as follows:

$$\begin{aligned} \Gamma_2 = & -d\Delta u_2 + d\Delta u_1 - k_2 e_2^u \\ & -g_{syn}(u_1 - V_{syn}) \frac{1}{1 + \exp(-\lambda(u_1 - \theta_{syn}))} \\ & +g_{syn}(u_1 - V_{syn}) \frac{1}{1 + \exp(-\lambda(u_2 - \theta_{syn}))} \\ & , \end{aligned} \tag{27}$$

with the updated rule defined as follows:

$$k_{2t} = r_2 (e_2^u)^2, \tag{28}$$

where r_2 is a arbitrary positive constant.

Note that (27) and (28) are constructed as the proposed controller (10) and the updated rule (11).

Let $|e_2^u| + |e_2^v| + |e_2^w| = |u_2 - u_1| + |v_2 - v_1| + |w_2 - w_1|$ be the identical synchronization error of the network (26). We say that this network identically synchronizes if the identical synchronization error reaches zero as t approaches infinity.

First, we check the effectiveness of the proposed controller for this example in the following domain:

$$[0; T] \times \Omega = [0; 5000] \times [0; 100],$$

i.e., $\Omega \subset \mathbb{R}$ with Neumann zero flux boundary conditions. Besides, the initial conditions for the first node are defined as follows:

$$u_1(x, 0) = 1 + \cos(2\pi x),$$

$$v_1(x, 0) = 1 + \cos(2\pi x),$$

$$w_1(x, 0) = 1 + \cos(2\pi x),$$

for all $x \in \Omega$.

The initial conditions for the second node are defined so that the value is 0 everywhere, except at the central point, where we set the value to 1.

Fig. 8 illustrates the identical synchronization errors in the network described by system (25) with a coupling strength of $g_{syn} = 0.0005$. Specifically, in panel (a) of Fig. 8, we simulate the network without the controller given by equation (27) and the updated rule described in (28). The simulation results indicate that the identical synchronization error does not converge to zero, signifying that identical synchronization does not occur.

Fig. 9 displays the time series for all variables in the system defined by system (25), again without the controller from (27) and the updated rule from (28). In panel (a) of Fig. 9, the variable u_1 is represented by a solid line, while u_2 is shown with a dotted line. Similarly, panel (b) displays v_1 and v_2, and panel (c) shows w_1 and w_2. It is evident that the solid lines do not mimic the behavior of the dotted

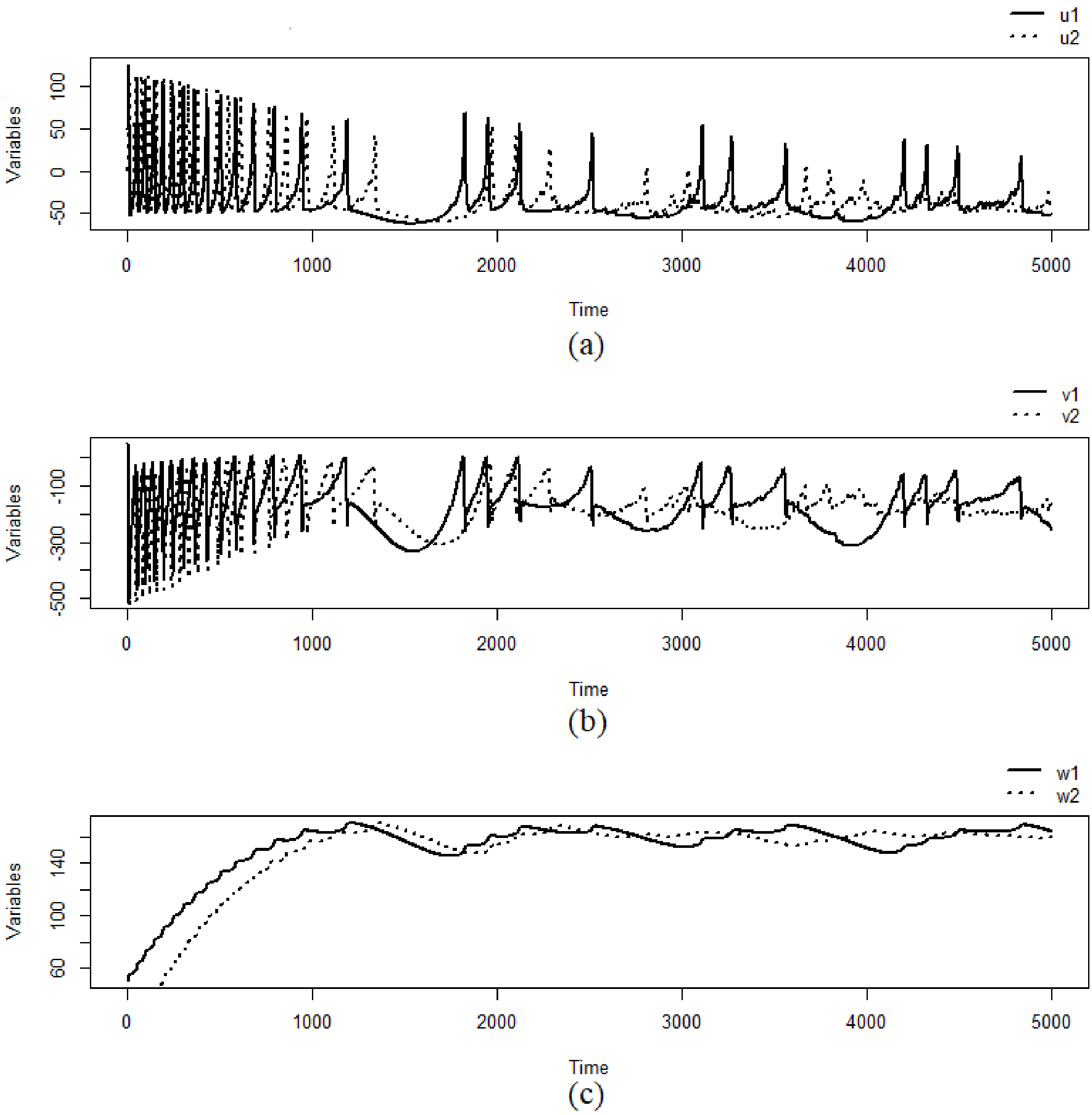

Fig. 3. The time series for all variables in the system described by system (21) without the controller referenced in (23) and the updated rule from (24).

lines, further confirming that identical synchronization does not occur in this scenario.

In Fig. 8(b), we simulate the network described by system (25) using the controller from equation (27) and the updated rule from equation (28), with $r_2 = 0.01$. This corresponds to the system outlined in system (26). The simulation results indicate that the identical synchronization error approaches zero, which implies the following relationships hold true:

$$u_1(x,t) \approx u_2(x,t),\ v_1(x,t) \approx v_2(x,t),\ w_1(x,t) \approx w_2(x,t).$$

Fig. 10 displays the time series for all variables of the system described by system (25) under the aforementioned controller and updated rule. In Fig. 10(a), the variable u_1 is represented by a solid line, while u_2 is shown as a dotted line. Similarly, Fig. 10(b) presents v_1 and v_2 with solid and dotted lines, respectively, and Fig. 10(c) does the same for w_1 and w_2. The results show that the solid lines mirror the behavior of the dotted lines, indicating that identical synchronization occurs in this scenario.

Next, we check the effectiveness of the proposed controller for this example in the following domain:

$$[0;T] = [0;500]\,;\ \Omega = [0;1] \times [0;1]\,,$$

i.e., $\Omega \subset \mathbb{R}^2$ with Neumann zero flux boundary conditions. Besides, the initial conditions for the first node are defined as follows:

$$u_1(x,0) = -(x_1-1)^2 - (x_2-1)^2,$$
$$v_1(x,0) = -(x_1-1)^2 - (x_2-1)^2,$$
$$w_1(x,0) = -(x_1-1)^2 - (x_2-1)^2,$$

for all $x = (x_1, x_2) \in \Omega$.

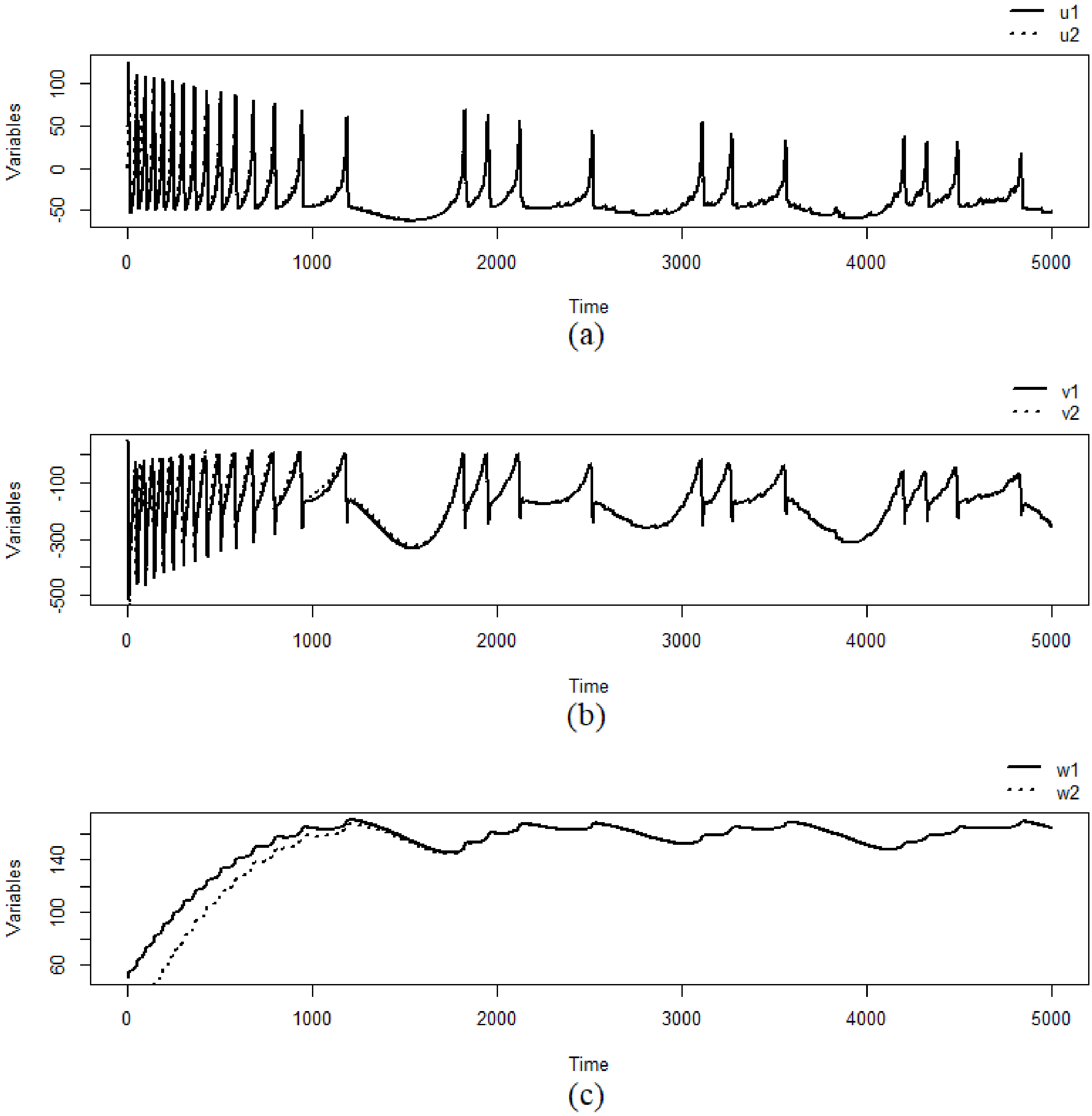

Fig. 4. The time series for all variables in the system (21) with the controller described in (23) and the updated rule in (24).

The initial conditions for the second node are defined as follows:

$$u_2(x,0) = -x_1^2 - x_2^2,$$
$$v_2(x,0) = -x_1^2 - x_2^2,$$
$$w_2(x,0) = -x_1^2 - x_2^2,$$

for all $x = (x_1, x_2) \in \Omega$.

Fig. 11 represents the identical synchronization errors of the network (25) concerning the coupling strength $g_{syn} = 0.0005$. Specifically, in Fig. 11(a), we simulate the network (25) without controller (27) and the updated rule (28). The simulation shows that the identical synchronization error does not reach zero, which means the identical synchronization phenomenon does not occur. Fig. 12 represents the patterns of all state variables of the system (25) without controller (27) and the updated rule (28) in Ω. Specifically, Fig. 12(a) represents the pattern of $u_1(x, 500)$, for all $x = (x_1, x_2) \in \Omega$ (respectively, $v_1(x, 500)$ in Fig. 12(b); $w_1(x, 500)$ in Fig. 12(c); $u_2(x, 500)$ in Fig. 12(d); $v_2(x, 500)$ in Fig. 12(e); $w_2(x, 500)$ in Fig. 12(f)). We can see that the pattern of $u_1(x, 500)$ and the pattern of $u_2(x, 500)$ are not the same (respectively, $v_1(x, 500)$ and $v_2(x, 500)$; $w_1(x, 500)$ and $w_2(x, 500)$). In other words, the identical synchronization phenomenon does not occur in this case.

However, in Fig. 11(b), we simulate the network (25) with controller (27) and the updated rule (28), i.e., the system (26). The simulation shows that the identical synchronization error reaches zero, which means:

$$u_1(x,t) \approx u_2(x,t),\ v_1(x,t) \approx v_2(x,t),\ w_1(x,t) \approx w_2(x,t).$$

Fig. 13 represents the patterns of all state variables of

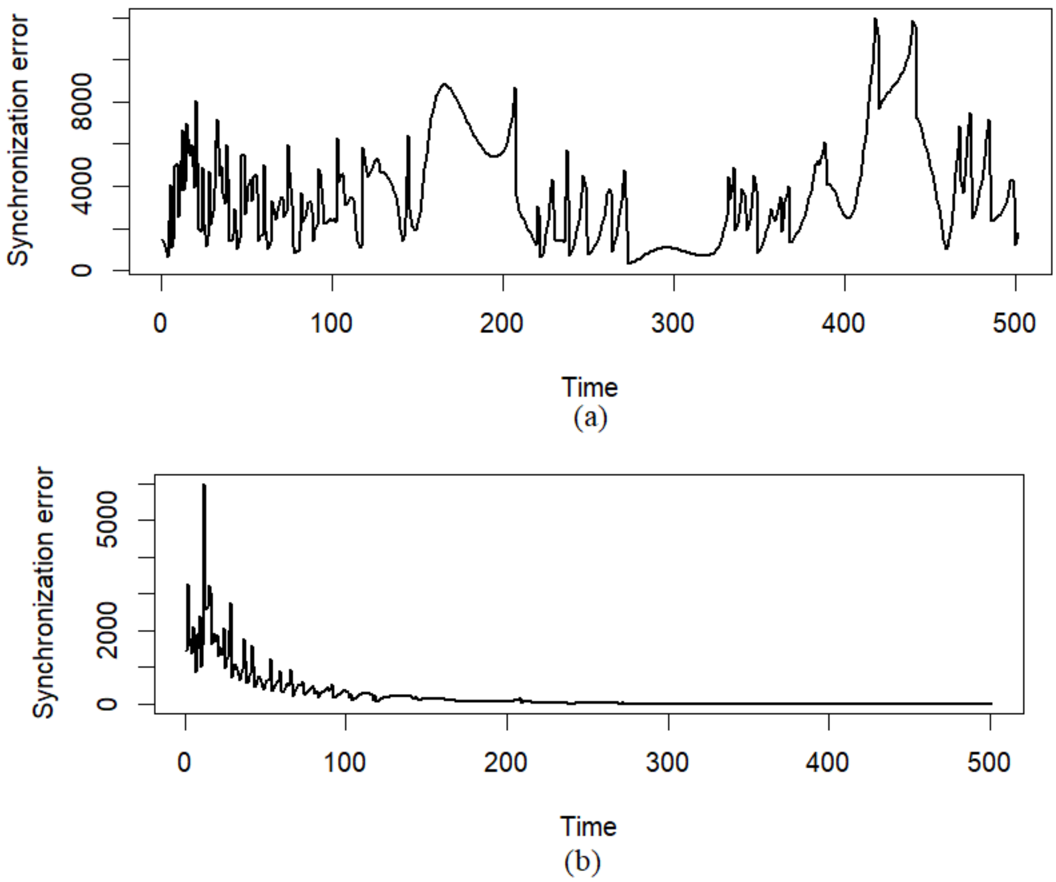

Fig. 5. Identical synchronization errors in the network (21) concerning the coupling strength $g_{syn} = 0.0005$, $\Omega = [0;1] \times [0;1] \subset \mathbb{R}^2$.

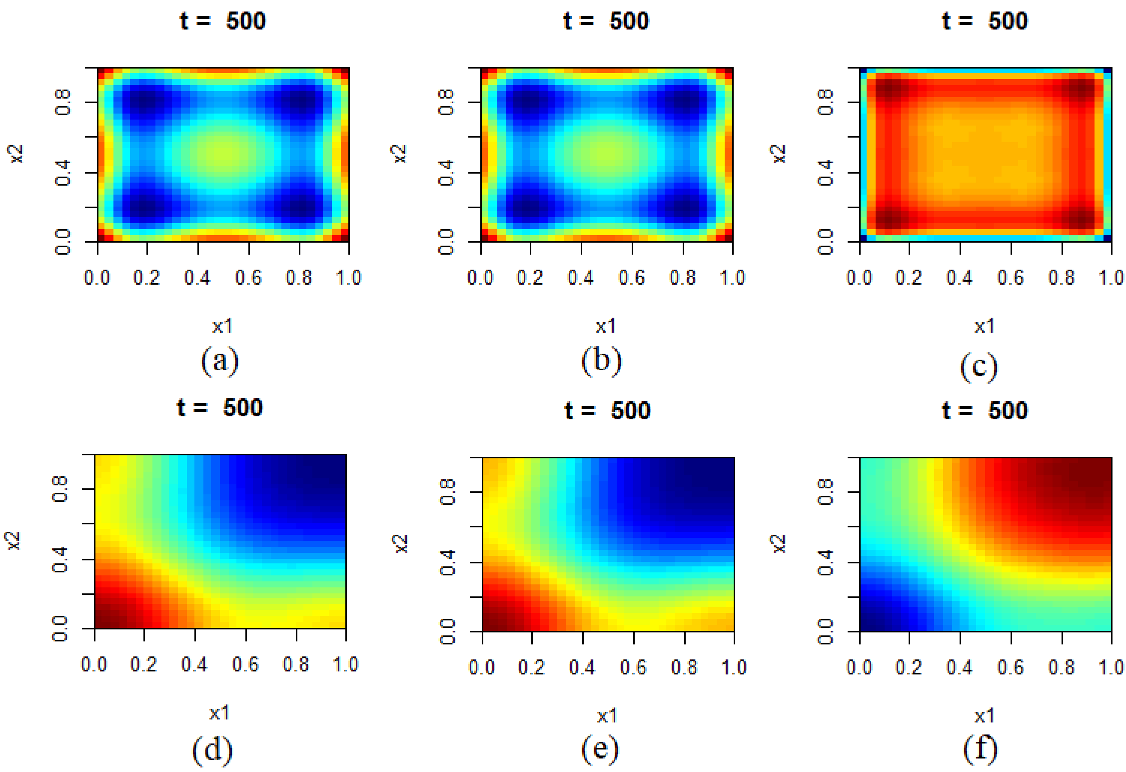

Fig. 6. The patterns of all state variables of the system described by (21) without the controller (23) and the updated rule (24) in the domain $\Omega = [0, 1] \times [0, 1]$.

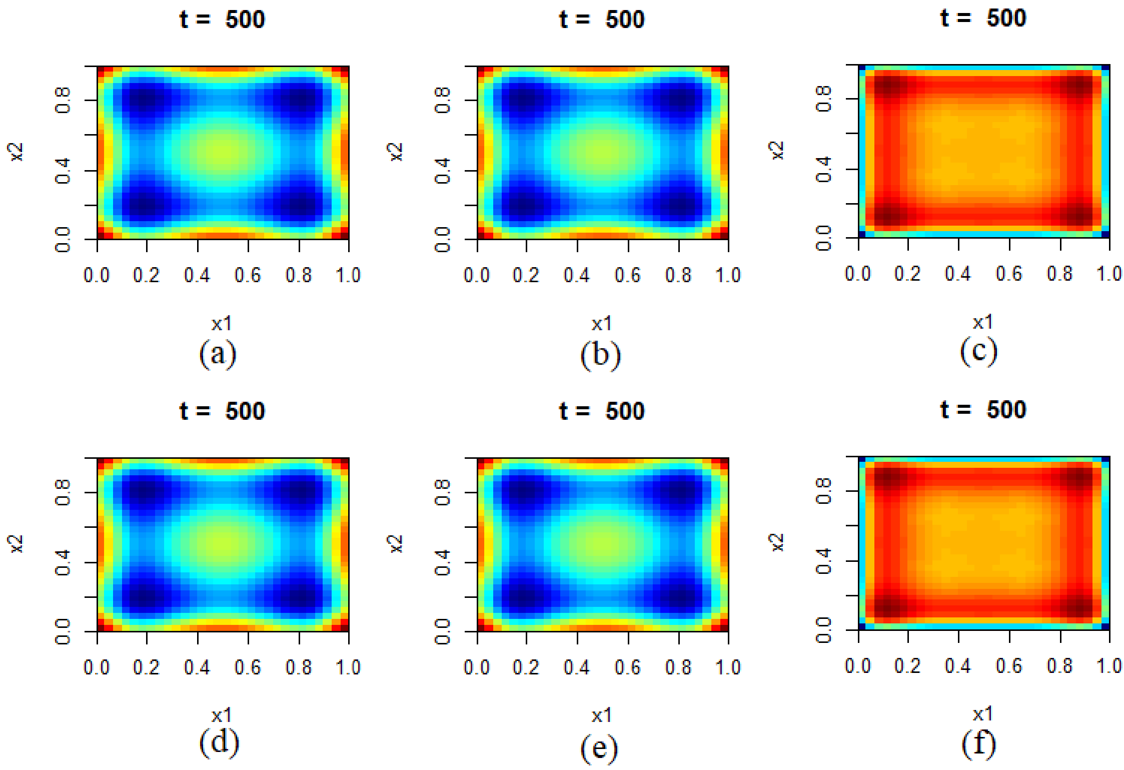

Fig. 7. The patterns of all state variables in the system described by (21), using the controller (23) and the updated rule (24), in the domain $\Omega = [0, 1] \times [0, 1]$.

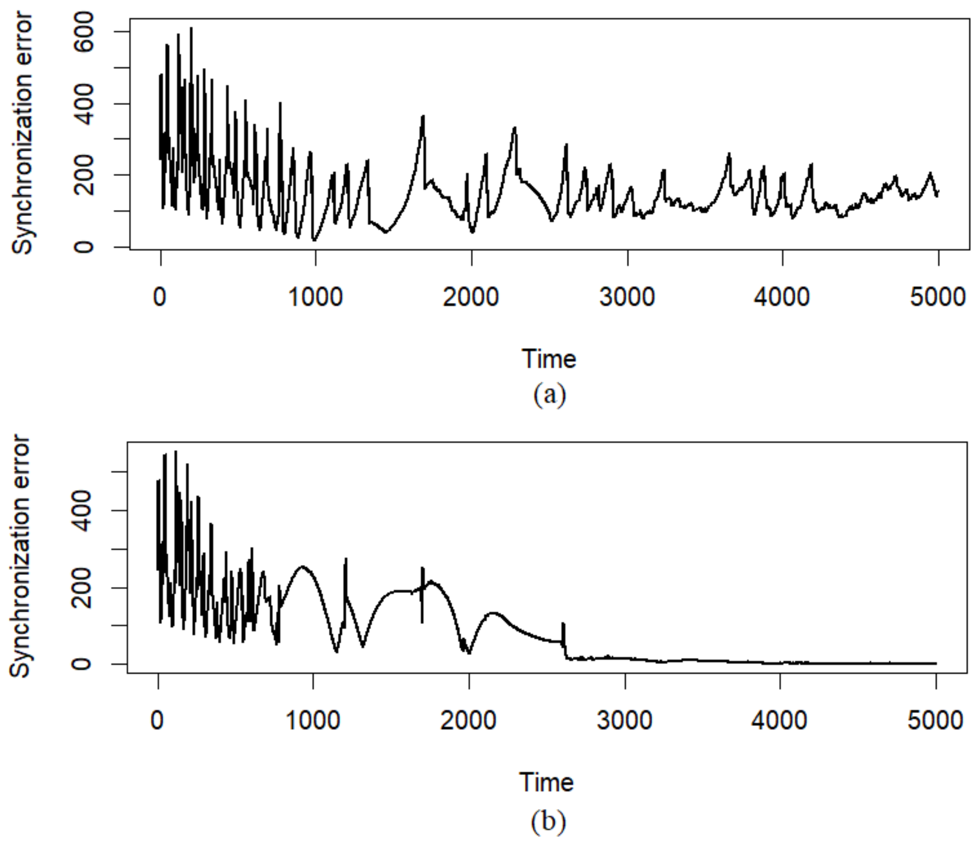

Fig. 8. Identical synchronization errors in the network (25) with respect to the coupling strength $g_{syn} = 0.0005$, $\Omega = [0; 100] \subset \mathbb{R}$.

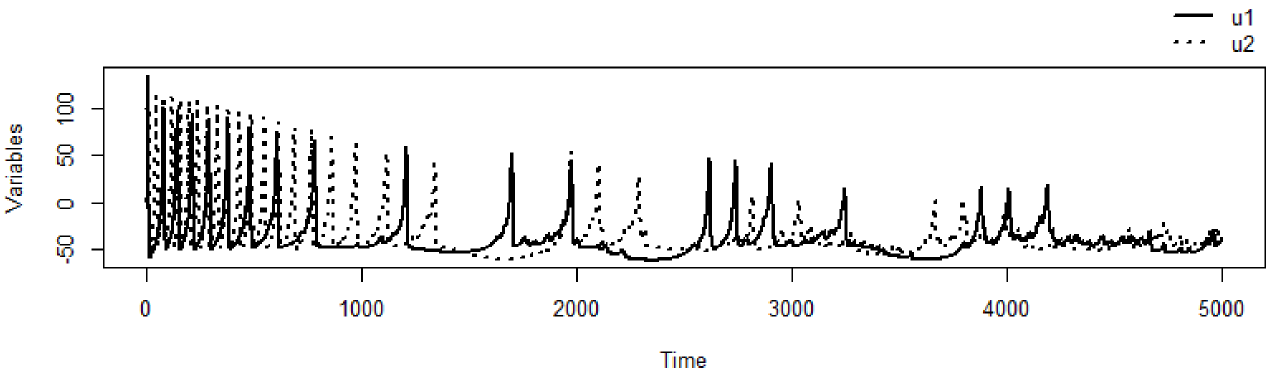

(a)

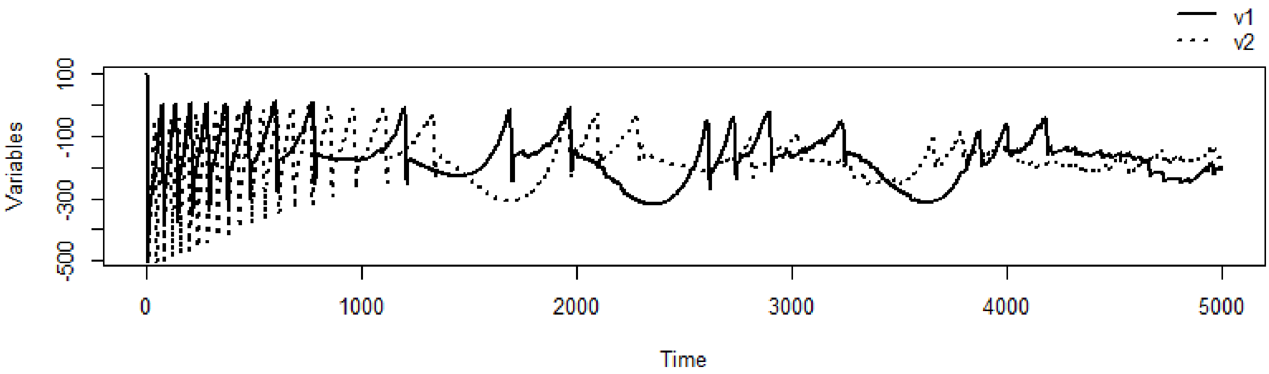

(b)

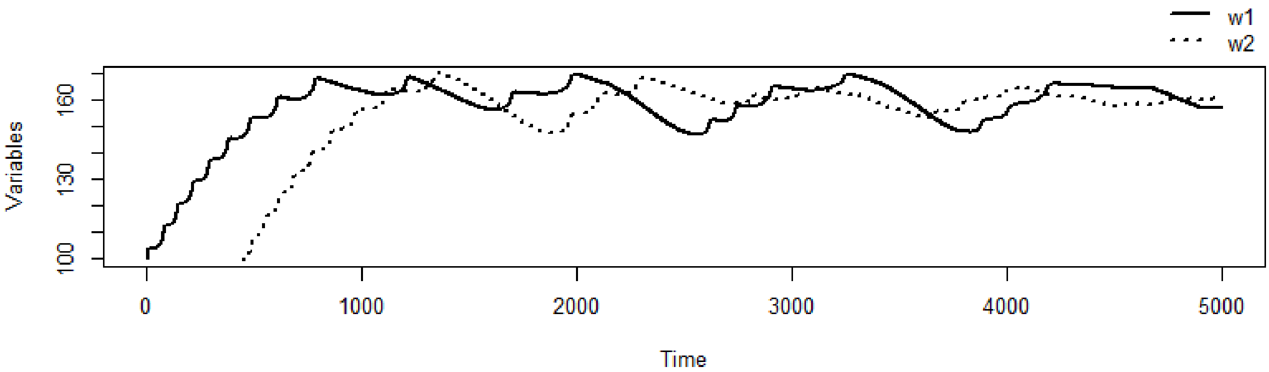

(c)

Fig. 9. The time series for all variables in the system described by (25) without the controller (27) and the updated rule (28).

the system (25) with controller (27) and the updated rule (28) in Ω. Specifically, Fig. 13(a) represents the pattern of $u_1(x, 500)$, for all $x = (x_1, x_2) \in \Omega$ (respectively, $v_1(x, 500)$ in Fig. 13(b); $w_1(x, 500)$ in Fig. 13(c); $u_2(x, 500)$ in Fig. 13(d); $v_2(x, 500)$ in Fig. 13(e); $w_2(x, 500)$ in Fig. 13(f)). We can see that the pattern of $u_1(x, 500)$ and the pattern of $u_2(x, 500)$ are the same (respectively, $v_1(x, 500)$ and $v_2(x, 500)$; $w_1(x, 500)$ and $w_2(x, 500)$). In other words, the identical synchronization phenomenon occurs in this case.

C. Example 3.

In this example, we will examine a network composed of four nodes that are linearly coupled, as illustrated in Fig. 14. In this figure, arrows indicate unidirectional coupling, while edges without arrows represent bidirectional coupling. To achieve identical synchronization, we will construct a controller based on the theoretical framework discussed earlier. Specifically, we will describe the system of the four-node network, structured as shown in Fig. 14, with linear

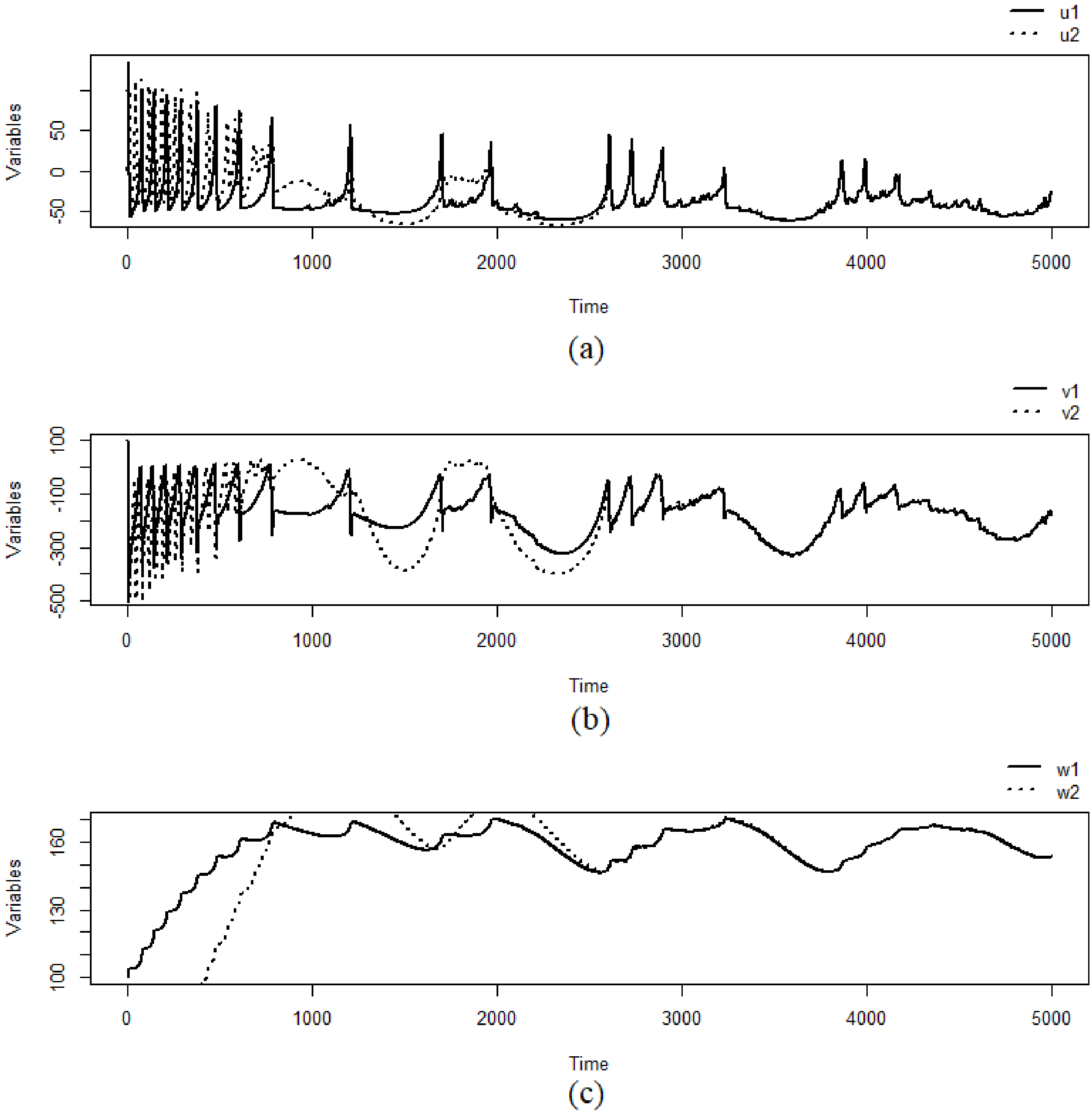

Fig. 10. The time series for all variables in the system (25), with the controller (27), along with the updated rule (28).

coupling as follows:

$$\begin{cases} u_{1t} = f(u_1) + v_1 - w_1 + I + d\Delta u_1 \\ \qquad\quad -g_{syn}(u_1 - u_2) - g_{syn}(u_1 - u_3), \\ v_{1t} = 1 - bu_1^2 - v_1, \\ w_{1t} = r(s(u_1 - c) - w_1), \\ u_{2t} = f(u_2) + v_2 - w_2 + I + d\Delta u_2 \\ \qquad\quad -g_{syn}(u_2 - u_1) - g_{syn}(u_2 - u_3), \\ v_{2t} = 1 - bu_2^2 - v_2, \\ w_{2t} = r(s(u_2 - c) - w_2), \\ u_{3t} = f(u_3) + v_3 - w_3 + I + d\Delta u_3 \\ \qquad\quad -g_{syn}(u_3 - u_1) - g_{syn}(u_3 - u_2), \\ v_{3t} = 1 - bu_3^2 - v_3, \\ w_{3t} = r(s(u_3 - c) - w_3), \\ u_{4t} = f(u_4) + v_4 - w_4 + I + d\Delta u_4 \\ \qquad\quad -g_{syn}(u_4 - u_3), \\ v_{4t} = 1 - bu_4^2 - v_4, \\ w_{4t} = r(s(u_4 - c) - w_4). \end{cases} \tag{29}$$

Now, we construct a controller for this network as follows:

$$\begin{cases} u_{1t} = f(u_1) + v_1 - w_1 + I + d\Delta u_1 \\ \qquad\quad -g_{syn}(u_1 - u_2) - g_{syn}(u_1 - u_3), \\ v_{1t} = 1 - bu_1^2 - v_1, \\ w_{1t} = r(s(u_1 - c) - w_1), \\ u_{2t} = f(u_2) + v_2 - w_2 + I + d\Delta u_2 \\ \qquad\quad -g_{syn}(u_2 - u_1) - g_{syn}(u_2 - u_3) + \Gamma_2, \\ v_{2t} = 1 - bu_2^2 - v_2, \\ w_{2t} = r(s(u_2 - c) - w_2), \\ u_{3t} = f(u_3) + v_3 - w_3 + I + d\Delta u_3 \\ \qquad\quad -g_{syn}(u_3 - u_1) - g_{syn}(u_3 - u_2) + \Gamma_3, \\ v_{3t} = 1 - bu_3^2 - v_3, \\ w_{3t} = r(s(u_3 - c) - w_3), \\ u_{4t} = f(u_4) + v_4 - w_4 + I + d\Delta u_4 \\ \qquad\quad -g_{syn}(u_4 - u_3) + \Gamma_4, \\ v_{4t} = 1 - bu_4^2 - v_4, \\ w_{4t} = r(s(u_4 - c) - w_4). \end{cases} \tag{30}$$

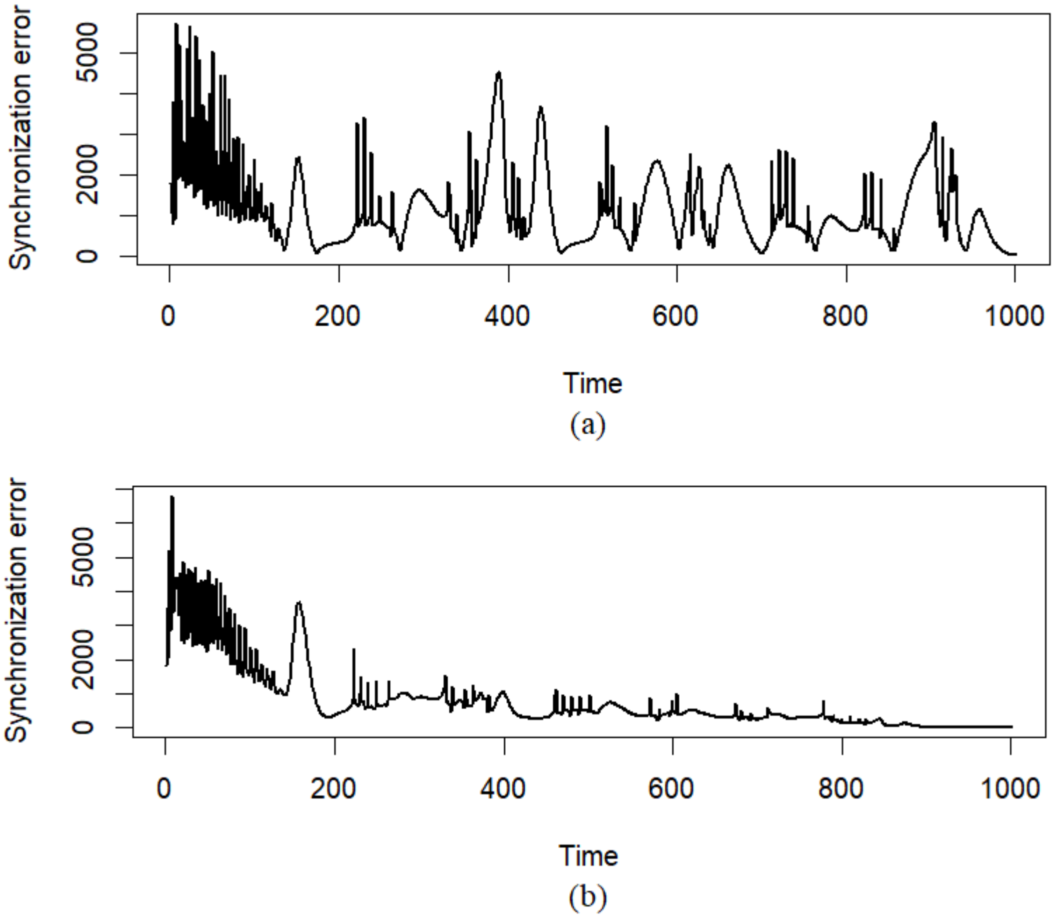

Fig. 11. Identical synchronization errors within the network described by (25) concerning the coupling strength $g_{syn} = 0.0005$, $\Omega = [0; 1] \times [0; 1] \subset \mathbb{R}^2$.

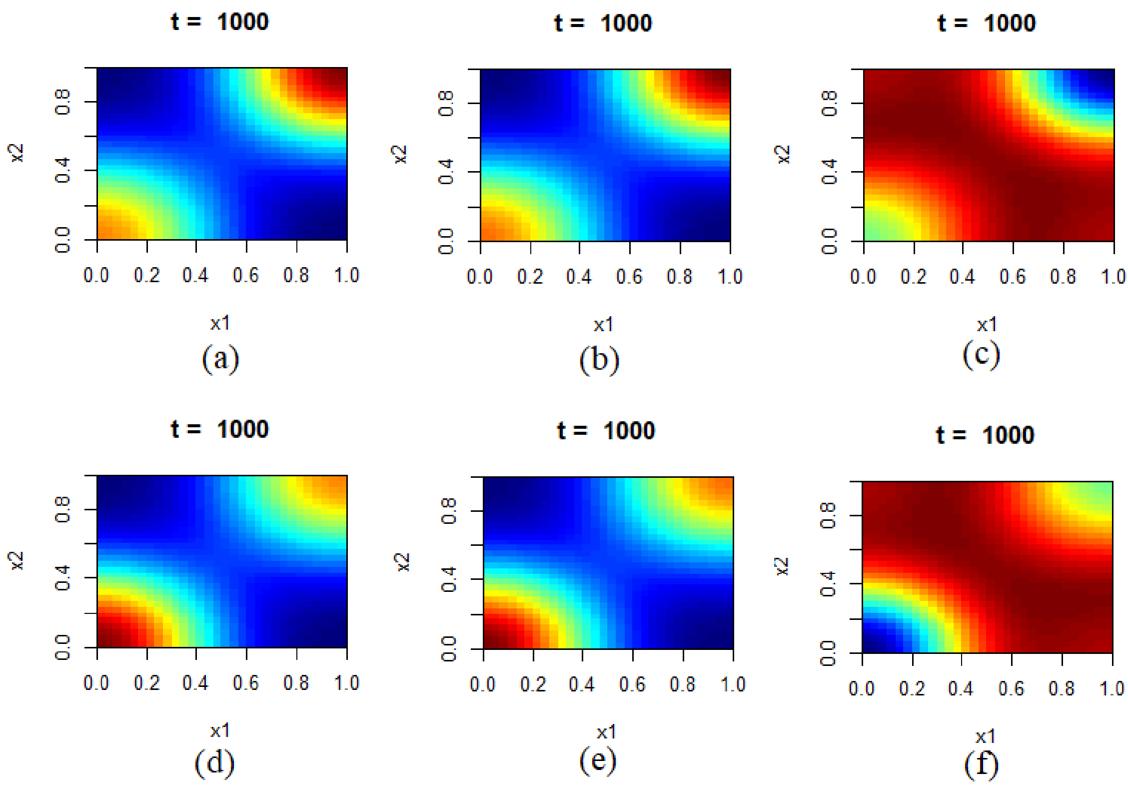

Fig. 12. The patterns of all state variables of the system described by (25), without the controller (27) and following the updated rule (28), over the region $\Omega = [0, 1] \times [0, 1]$.

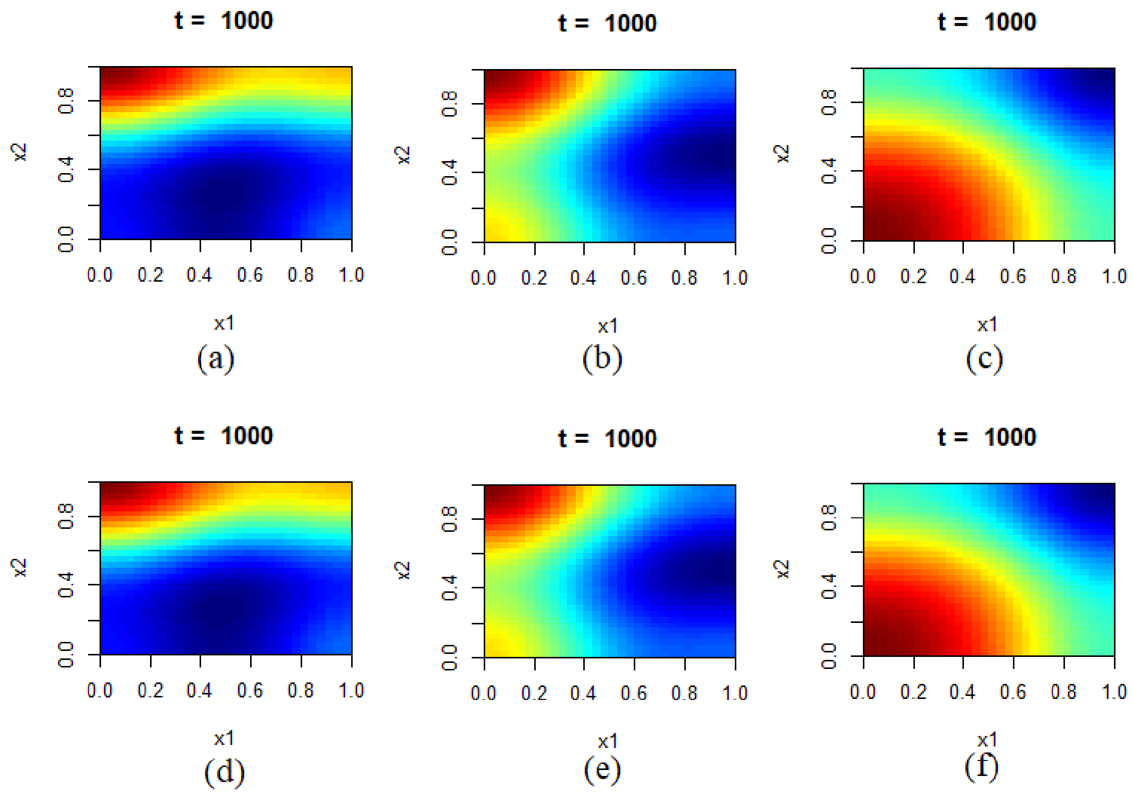

Fig. 13. The patterns of all state variables in the system (25) with the controller (27) and the updated rule (28), in the domain $\Omega = [0, 1] \times [0, 1]$.

where the controller Γ_2 is designed as follows:

$$\begin{cases} \Gamma_2 = -d\Delta u_2 + d\Delta u_1 + g_{syn}(u_1 - u_3) \\ \qquad -g_{syn}(u_1 - u_2) - g_{syn}(u_1 - u_3) - k_2 e_2^u, \\ \Gamma_3 = -d\Delta u_3 + d\Delta u_1 + g_{syn}(u_1 - u_2) \\ \qquad -g_{syn}(u_1 - u_2) - g_{syn}(u_1 - u_3) - k_3 e_3^u, \\ \Gamma_4 = -d\Delta u_4 + d\Delta u_1 + g_{syn}(u_1 - u_3) \\ \qquad -g_{syn}(u_1 - u_2) - g_{syn}(u_1 - u_3) - k_4 e_4^u, \end{cases} \tag{31}$$

with the updated rule defined as follows:

$$\begin{cases} k_{2t} = r_2 (e_2^u)^2, \\ k_{3t} = r_3 (e_3^u)^2, \\ k_{4t} = r_4 (e_4^u)^2. \end{cases} \tag{32}$$

where r_2, r_3, r_4 are arbitrary positive constants.

Note that (31) and (32) are constructed as the proposed controller (10) and the updated rule (11).

Let $\sum_{i=2}^{4} |e_i^u| + |e_i^v| + |e_i^w| = \sum_{i=2}^{4} |u_i - u_1| + |v_i - v_1| + |w_i - w_1|$ be the identical synchronization error of the network (29). We say that this network identically synchronizes if the identical synchronization error reaches zero as t approaches infinity.

First, we check the effectiveness of the proposed controller for this example in the following domain:

$$[0; T] \times \Omega = [0; 5000] \times [0; 100],$$

i.e., $\Omega \subset \mathbb{R}$ with Neumann zero flux boundary conditions. Besides, the initial conditions for the first node are defined as follows:

$$u_1(x, 0) = 1 + \sin(2\pi x),$$

$$v_1(x, 0) = 1 + \sin(2\pi x),$$

$$w_1(x, 0) = 1 + \sin(2\pi x),$$

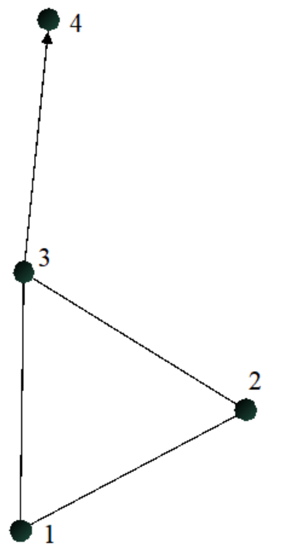

Fig. 14. An example of a graph with four nodes arranged in an arbitrary structure.

for all $x \in \Omega$.

The initial conditions for the second node are defined such that the value is 0 everywhere except at the central point, where we set the value to 1.

The initial conditions for the third node are defined as follows:

$$u_3(x, 0) = \sin(2\pi x),$$

$$v_3(x, 0) = \sin(2\pi x),$$

$$w_3(x, 0) = \sin(2\pi x),$$

for all $x \in \Omega$.

The initial conditions for the fourth node are defined as follows:

$$u_4(x,0) = 1 + \cos(2\pi x),$$
$$v_4(x,0) = 1 + \cos(2\pi x),$$
$$w_4(x,0) = 1 + \cos(2\pi x),$$

for all $x \in \Omega$.

Fig. 15 illustrates the identical synchronization errors of the network described by system (29) with a coupling strength of $g_{syn} = 0.0005$. In panel (a) of Fig. 15, we simulate the network (29) without the controller specified in (31) and the updated rule presented in (32). The results indicate that the identical synchronization error does not reach zero, suggesting that identical synchronization does not occur in this scenario.

Conversely, in panel (b) of Fig. 15, we simulate the network (29) with the controller from (31) and the updated rule from (32), using parameters $r_2 = 0.2$, $r_3 = 0.3$, and $r_4 = 0.4$, corresponding to system (30). The simulation results show that the identical synchronization error reaches zero. This indicates that identical synchronization occurs in this case.

Next, we check the effectiveness of the proposed controller for this example in the following domain:

$$[0;T] = [0;500]\,;\ \Omega = [0;1] \times [0;1]\,,$$

i.e., $\Omega \subset \mathbb{R}^2$ with Neumann zero flux boundary conditions. Besides, the initial conditions for the first node are defined as follows:

$$u_1(x,0) = -(x_1 - 0.5)^2 - (x_2 - 0.5)^2,$$
$$v_1(x,0) = -(x_1 - 0.5)^2 - (x_2 - 0.5)^2,$$
$$w_1(x,0) = -(x_1 - 0.5)^2 - (x_2 - 0.5)^2,$$

for all $x = (x_1, x_2) \in \Omega$.

The initial conditions for the second node are defined as follows:

$$u_2(x,0) = -x_1^2 - x_2^2,$$
$$v_2(x,0) = -x_1^2 - x_2^2,$$
$$w_2(x,0) = -x_1^2 - x_2^2,$$

for all $x = (x_1, x_2) \in \Omega$.

The initial conditions for the third node are defined as follows:

$$u_3(x,0) = -(x_1 - 0.5)^2 - (x_2 - 0.5)^2,$$
$$v_3(x,0) = -(x_1 - 0.5)^2 - (x_2 - 0.5)^2,$$
$$w_3(x,0) = -(x_1 - 0.5)^2 - (x_2 - 0.5)^2,$$

for all $x = (x_1, x_2) \in \Omega$.

The initial conditions for the fourth node are defined as follows:

$$u_4(x,0) = -x_1^2 - x_2^2,$$
$$v_4(x,0) = -x_1^2 - x_2^2,$$
$$w_4(x,0) = -x_1^2 - x_2^2,$$

for all $x = (x_1, x_2) \in \Omega$.

Fig. 5 illustrates the identical synchronization errors of the network described in (29) with a coupling strength of $g_{syn} = 0.0005$. In Figure 16(a), we simulate the network (29) without the controller (31) and the updated rule (32). The simulation results indicate that the identical synchronization error does not converge to zero, implying that the identical synchronization phenomenon does not occur in this scenario.

Conversely, in Figure 5(b), we simulate the network (29) with the controller (31) and the updated rule (32), representing the system outlined in (30). The results show that the identical synchronization error reaches zero, indicating that the identical synchronization phenomenon does indeed occur in this case.

Remark 3. The examples provided demonstrate that in both cases, where $\Omega \subset \mathbb{R}$ and $\Omega \subset \mathbb{R}^2$, achieving identical synchronization is not possible without the proposed controller discussed in the theoretical section. When utilizing this controller, the synchronization error defined in $\mathbb{R}$ approaches zero as time t increases significantly.

It is important to note that while the networks investigated in this study can achieve identical synchronization with a large enough value of coupling strength [15], [16], [18], the resulting synchronization error in those cases theoretically does not remain within $\mathbb{R}$. This study offers a significant advantage over previous works by the author, as it ensures that the synchronization error is indeed within $\mathbb{R}$. Moreover, under the same conditions, the network with the controller achieves identical synchronization more effectively than a network without one. In summary, the numerical results are consistent with the theoretical findings.

IV. Conclusion

This paper examines identical synchronization in networks featuring arbitrary topological structures composed of n reaction-diffusion systems of the Hindmarsh-Rose 3D type. We design a nonlinear adaptive controller and construct a suitable Lyapunov function to achieve the desired synchronization based on the identical synchronization error defined in $\mathbb{R}$. The numerical results demonstrate the effectiveness of the proposed method. Specifically, identical synchronization is not achieved without the proposed controller, whereas the network successfully attains identical synchronization when this controller is implemented.

References

[1] M. A. Aziz-Alaoui, "Synchronization of Chaos", *Encyclopedia of Mathematical Physics, Elsevier*, Vol. 5, pp. 213-226, 2006.

[2] N. Corson, "Dynamics of a neural model, synchronization and complexity", *Thesis, University of Le Havre*, France, 2009.

[3] A. Pikovsky, M. Rosenblum and J. Kurths, "Synchronization, A Universal Concept in Nonlinear Science", *Cambridge University Press*, 2001.

[4] A. L. Hodgkin and A. F. Huxley, "A quantitative description of membrane current and its application to conduction and excitation in nerve", *J. Physiol.117*, pp. 500-544, 1952.

[5] J. D. Murray, "Mathematical Biology", *Springer*, 2010.

[6] E. M. Izhikevich, "Dynamical Systems in Neuroscience", *The MIT Press*, 2007.

[7] G. B. Ermentrout and D. H. Terman, "Mathematical Foundations of Neurosciences", *Springer*, 2009.

[8] J. P. Keener and J. Sneyd, "Mathematical Physiology", *Springer*, 2009.

[9] J. L. Hindmarsh and R. M Rose, "A model of the nerve impulse using two firstorder differential equations", *Nature*, vol. 296, pp. 162-164, 1982.

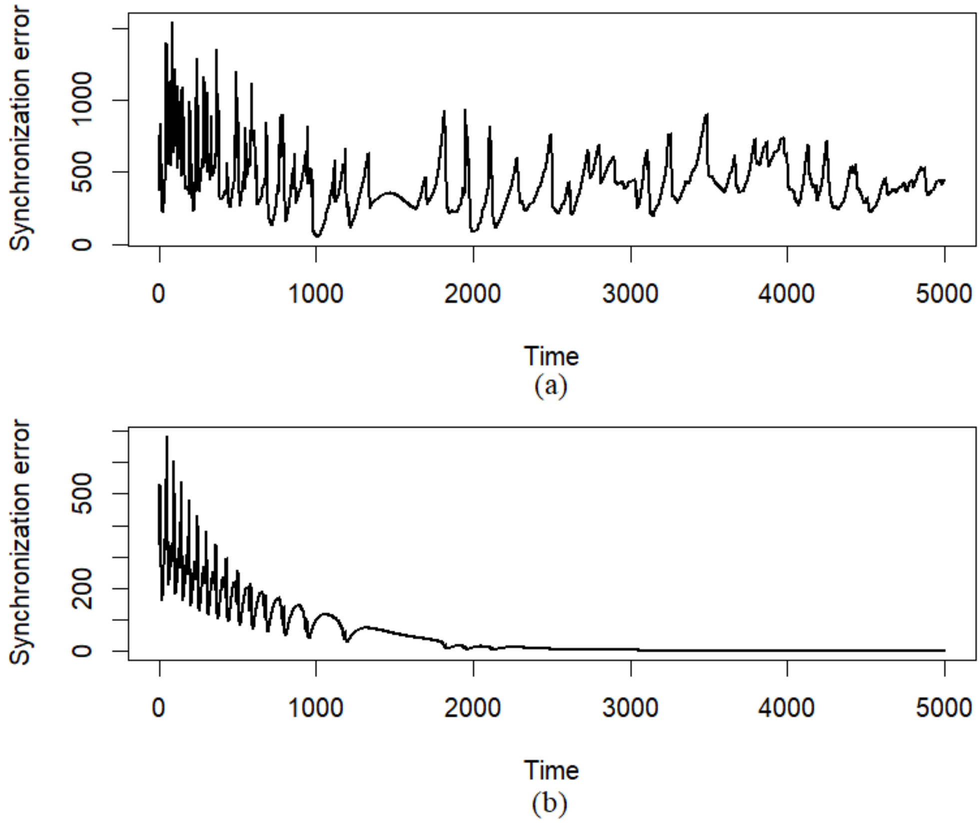

Fig. 15. Identical synchronization errors of the network described by (29) with respect to the coupling strength $g_{syn} = 0.0005$, $\Omega = [0; 100] \subset \mathbb{R}$.

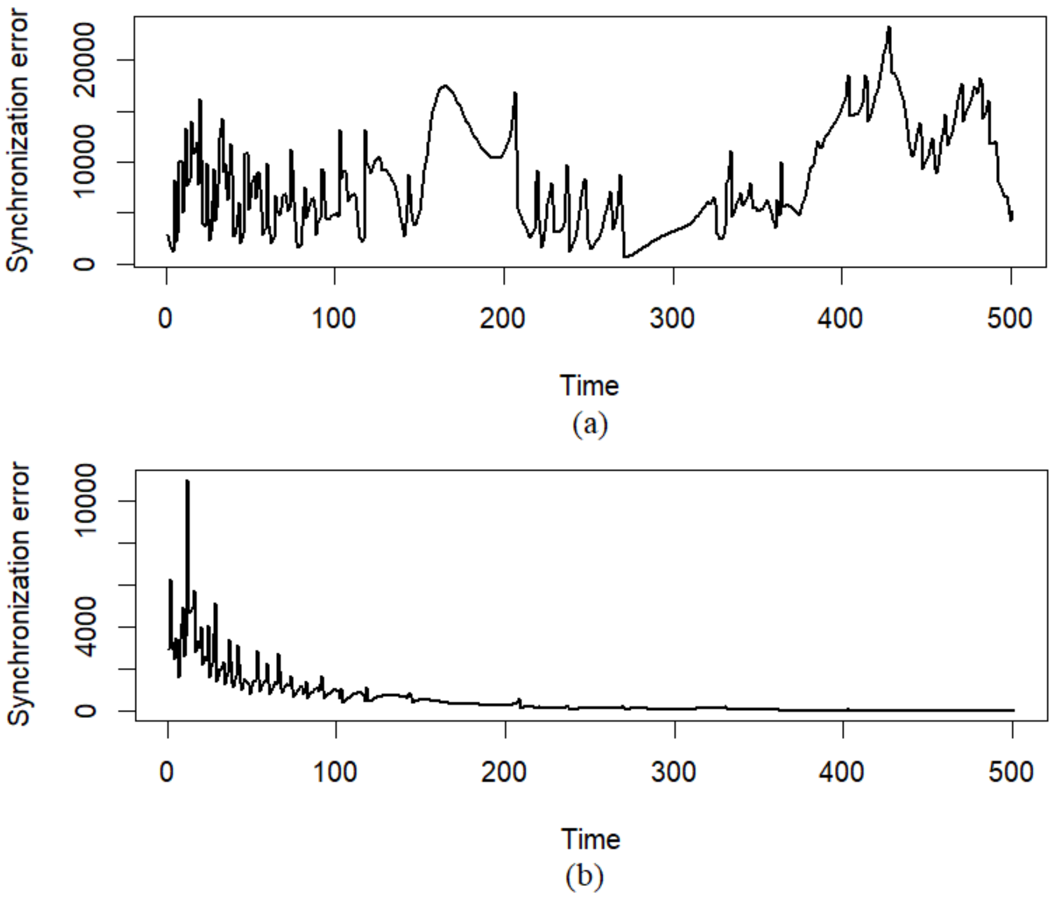

Fig. 16. Identical synchronization errors in the network described by (29) with a coupling strength of $g_{syn} = 0.0005$, $\Omega = [0; 1] \times [0; 1] \subset \mathbb{R}^2$.

[10] B. Ambrosio and M. A. Aziz-Alaoui, ”Synchronization and control of coupled reaction-diffusion systems of the FitzHugh-Nagumo-type”, *Computers and Mathematics with Applications*, vol 64, pp. 934-943, 2012.

[11] B. Ambrosio and M. A. Aziz-Alaoui, ”Synchronization and control of a network of coupled reaction-diffusion systems of generalized FitzHugh-Nagumo type”, *ESAIM: Proceedings*, Vol. 39, pp. 15-24, 2013.

[12] B. Ambrosio, M. A. Aziz-Alaoui, and V. L. E. Phan, ” Global attractor of complex networks of reaction-diffusion systems of Fitzhugh-Nagumo type”, *American Institute of Mathematical Sciences, Discrete and Continuous Dynamical Systems-Series B,* **23**(9), 3787-3797, 2018.

[13] D. Aeyels, ”Asymptotic Stability of Nonautonomous Systems by Lyapunov’s Direct Method”, *Systems and Control Letters,* 25, 273-280, 1995.

[14] I. Belykh, E. De Lange and M. Hasler, ”Synchronization of bursting neurons: What matters in the network topology”, *Phys. Rev. Lett.* 188101, 2005.

[15] V. L. E. Phan, ”Sufficient Condition for Synchronization in Complete Networks of Reaction-Diffusion Equations of Hindmarsh-Rose Type with Linear Coupling”, *IAENG International Journal of Applied Mathematics*, vol. 52, no. 2, pp. 315-319, 2022.

[16] V. L. E. Phan, ”Sufficient Condition for Synchronization in Complete Networks of n Reaction-Diffusion Systems of Hindmarsh-Rose Type with Nonlinear Coupling”, *Engineering Letters*, vol. 31, no. 1, pp413-418, 2023.

[17] V. L. E. Phan, ”Global Attractor of Networks of n Coupled Reaction-Diffusion Systems of Hindmarsh-Rose Type”, *Engineering Letters,* vol. 31, no. 3, pp1215-1220, 2023.

[18] V. L. E. Phan, ”Sufficient Conditions for Identical Synchronization in the Networks Constructed by Levels of n Reaction-Diffusion Systems of Hindmarsh-Rose Type with Linear Coupling”, *IAENG International Journal of Computer Science,* vol. 51, no. 4, pp430-436, 2024.

[19] V. L. E. Phan, ”Synchronous Controller between Drive Network of n Reaction-Diffusion Systems of FitzHugh - Nagumo type and Response Network of n Reaction-Diffusion Systems of Hindmarsh-Rose type,” *IAENG International Journal of Applied Mathematics,* vol. 54, no. 10, pp2049-2059, 2024.

[20] S. Stogatz and I. Stewart, ”Coupled Oscillators and Biological Synchronization”, *Scientific American,* 269, 102-109, 1993.

[21] S. H. Strogatz, ”Exploring Complex Networks”, *Nature,* 410, 268-276, 2001.

[22] Q. Xie, R.G. Chen and E. Bolt, ”Hybrid Chaos Synchronization and Its Application in Information Processing”, *Mathematical and Computer Modelling,* 1, 145-163, 2002.

[23] C.M. Gray, ”Synchronous Oscillations in Neural Systems”, *Journal of Computational Neuroscience,* 1, 11-38, 1994.